The acid-induced folded state of Sac7d is the native state

JENNIFER L. BEDELL, BRADFORD S. McCRARY, STEPHEN P. EDMONDSON,
AND JOHN W. SHRIVER

Department of Biochemistry and Molecular Biology, School of Medicine, Southern Illinois University, Carbondale, Illinois 62901

Abstract

Sac7d unfolds at low pH in the absence of salt, with the greatest extent of unfolding obtained at pH 2. We have previously shown that the acid unfolded protein is induced to refold by decreasing the pH to 0 or by addition of salt (McCrary BS, Bedell J, Edmondson SP, Shriver JW, 1998, *J Mol Biol 276*:203–224). Both near-ultraviolet circular dichroism spectra and ANS fluorescence enhancements indicate that the acid- and salt-induced folded states have a native fold and are not molten globular. ^{1}H,^{15}N heteronuclear single quantum coherence NMR spectra confirm that the native, acid-, and salt-induced folded states are essentially identical. The most significant differences in amide ^{1}H and ^{15}N chemical shifts are attributed to hydrogen bonding to titrating carboxyl side chains and through-bond inductive effects. The ^{1}H NMR chemical shifts of protons affected by ring currents in the hydrophobic core of the acid- and salt-induced folded states are identical to those observed in the native. The radius of gyration of the acid-induced folded state at pH 0 is shown to be identical to that of the native state at pH 7 by small angle X-ray scattering. We conclude that acid-induced collapse of Sac7d does not lead to a molten globule but proceeds directly to the native state. The folding of Sac7d as a function of pH and anion concentration is summarized with a phase diagram that is similar to those observed for other proteins that undergo acid-induced folding except that the A-state is encompassed by the native state. These results demonstrate that formation of a molten globule is not a general property of proteins that are refolded by acid.

Keywords: anion binding; ANS binding; circular dichroism; hyperthermophile; molten globule; NMR; small-angle X-ray scattering; *Sulfolobus*
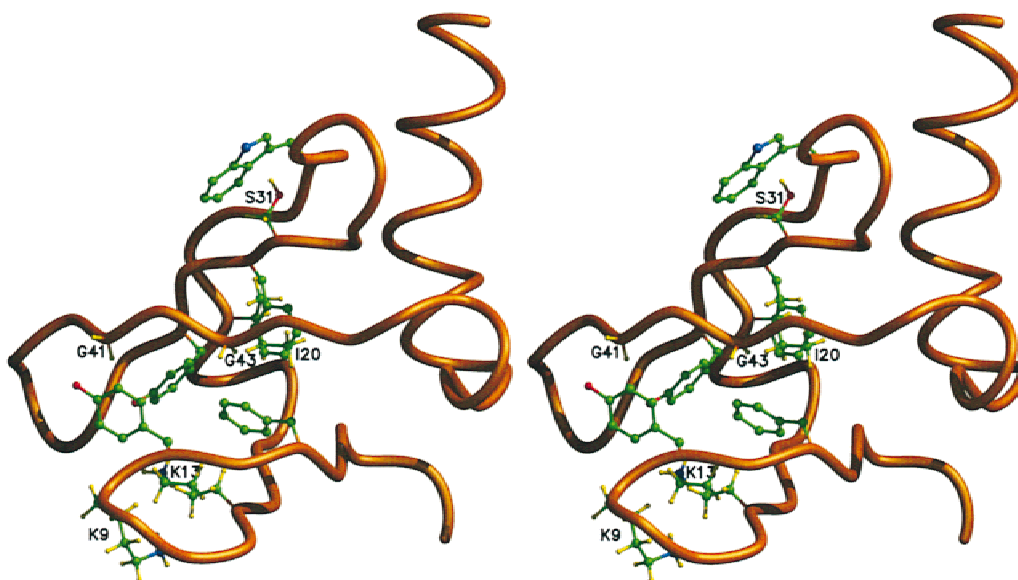
Proteins are commonly destabilized by acid with maximal unfolding typically occurring near pH 2 (Linderström-Lang, 1924; Tanford, 1970; Matthew et al., 1985; Yang & Honig, 1993; Oliveberg et al., 1994; Garcia-Moreno, 1995). In many cases, a further decrease in pH, or the addition of salt, leads to a collapse of the unfolded chain into a compact "denatured" state referred to as the acid or A-state (Goto et al., 1990; Fink et al., 1994). The A-state is stabilized by anions contributed from either acid or salt. It has been shown to exist for a diverse array of proteins ranging from nearly all α-helical to largely all β-sheet (Fink et al., 1994). In every instance described to date, the properties of the A-state have been those of the so-called molten globule (Ptitsyn, 1987, 1995; Kuwajima, 1989; Fink et al., 1994; Fink, 1995), i.e., a folded intermediate with native-like secondary structure as indicated by the far-UV CD spectrum, but an expanded structure with a radius of gyration approximately 10–20% greater than that of the native state, loss of close packing tertiary contacts as indicated by the absence of near-UV CD and NMR chemical shift dispersion, and exposure of hydrophobic patches as indicated by enhanced fluorescence of the dye ANS. The acid-induced molten globule appears to be a native-like structure that has been forced to expand due to electrostatic repulsion and therefore represents a folded protein in which the close packing of the core has been prevented. As such, it is thought by many to resemble an "on pathway" intermediate in protein folding that might occur prior to the final reinforcement of the native cooperative structure (Ptitsyn et al., 1990; Baldwin, 1991; Jennings & Wright, 1993). If the molten globule is a general intermediate in protein folding, it should be possible to generate such a structure for any protein. It has therefore been proposed to be a general physical state of globular proteins (Ohgushi & Wada, 1983; Goto & Fink, 1990; Ptitsyn et al., 1990; Stigter et al., 1991; Haynie & Freire, 1993; Sanz et al., 1994; Fink, 1995).

Although molten globules can be formed by various perturbations of the native state, the acid-induced folded states have been the most commonly studied species. However, there has been rel-

Fig. 1. Schematic representation of the solution structure of Sac7d (Edmondson et al., 1995) showing the aromatic side chains and neighboring residues experiencing the most significant ring current effects.

atively little work on characterizing the structural basis for the formation of the acid-induced molten globule (Finkelstein & Shakhnovich, 1989; Goto et al., 1990; Goto & Nishikiori, 1991; Stigter et al., 1991; Haynie & Freire, 1993, 1994; Hagihara et al., 1994; Yang & Honig, 1994; Freire, 1995; Kay & Baldwin, 1998). It is not clear why stabilization of a protein by anion binding at low pH leads to an incompletely collapsed native structure, and not the native structure. We show here that in at least one case acid-induced folding of a protein is capable of achieving the native state.

Sac7d is a small (66 residue, 7,600 MW) DNA-binding protein from the thermoacidophile *Sulfolobus acidocaldarius*, an archaeon growing up to 85 °C in hot springs around the world (Brock et al., 1972; Grote et al., 1986; Stetter et al., 1990). The protein folds into a compact, globular monomer with a hydrophobic core of 10 side chains including two tyrosines and two phenylalanines (Fig. 1) (Edmondson et al., 1995). As might be expected for a chromatin protein, it is highly basic with 14 lysines, 4 arginines, 7 glutamates, and 5 aspartates. The protein has proven to be exceptionally well behaved for structural thermodynamic studies of the origin of hyperthermophile protein stability with a T_m at pH 7 of 90.7 °C and a maximal stability of 6.2 kcal/mol at 17 °C (McAfee et al., 1995; McCrary et al., 1996, 1998).

Results

Circular dichroism

Both the near- and far-UV CD spectra of Sac7d are pH dependent *in the absence of salt* and indicate protein unfolding with decreasing pH down to pH 2, and then refolding at lower pH (McCrary et al., 1998). The far-UV spectra indicate that maximal unfolding (viz. 75%) is obtained at pH 2 in the absence of added salt (McCrary et al., 1998). The near-UV spectra showed that tertiary con-

tacts are maintained in the remaining folded protein (Fig. 2). Addition of salt (0.3 M KCl) at pH 2 led to refolding and a near-UV CD spectrum essentially identical to that observed at higher pH (e.g., pH 3.5 and 5). Similarly, decreasing the pH to 0, either in the presence (Fig. 2) or absence (McCrary et al., 1998) of KCl, also led to refolding and a near-UV spectrum similar to that observed at high pH. For comparison, the near-UV CD spectrum was lost upon increasing the temperature to 99 °C at pH 0. Thus, Sac7d folding at pH 2 is promoted by either salt or acid, and the resulting structure appears to have native-like tertiary structure.
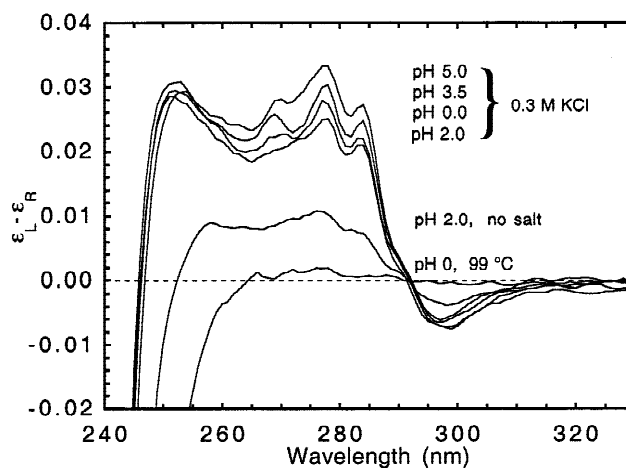
Fig. 2. Near-UV CD spectra of Sac7d (1 mg/mL) at pH 5.0, 3.5, 2.0, and 0.0 in 0.3 M KCl (0.01 M glycine at 25 °C). The CD spectrum at pH 2 in the absence of added salt is also shown along with thermally unfolded protein at pH 0 and 99 °C.

ANS fluorescence

ANS fluorescence has been used to detect the presence of hydrophobic regions in proteins (Stryer, 1965) and as a diagnostic indicator of the collapsed, molten globule state (Mulqeen & Kronman, 1982; Semisotnov et al., 1991). Although ANS binds to proteins through electrostatic interactions (Matulis & Lovrien, 1998), the fluorescence of ANS is enhanced by the presence of exposed hydrophobic regions. The fluorescence of ANS was unaffected by native Sac7d at pH 7 (Fig. 3). In the absence of salt at pH 2, where about 75% of Sac7d is unfolded, there was a sixfold enhancement of ANS fluorescence (at 500 nm). In contrast, the fluorescence of ANS was relatively unchanged in the presence of the acid- or salt-induced folded forms of Sac7d. Acid-induced folding (pH 0) led to a slight loss in fluorescence intensity while the salt induced folded form at pH 2 showed a 1.5 fold enhancement relative to the native at pH 7. Both acid- and salt-induced forms showed essentially the same negligible effect on ANS fluorescence enhancement as the native state, which indicates that the salt- and acid-induced folded states are not molten globular. As a control, we measured the effect of native and molten globule α-lactalbumin on ANS fluorescence (Fig. 3). Although ANS fluorescence was unaffected by the presence of the native state of α-lactalbumin at pH 7, formation of the molten globule by titration to pH 2 (Kuwajima et al., 1976; Fink et al., 1994) led to an 18-fold enhancement of the fluorescence intensity. (α-Lactalbumin is an example of a Type II protein in the classification scheme of Fink et al. (1994) in that addition of acid leads directly to the molten globule.) The molten globule of α-lactalbumin in the presence of salt (0.3 M KCl) showed a sixfold fluorescence enhancement over that observed for the native state.

Amide ^1H and ^{15}N chemical shifts

Amide ^1H and ^{15}N chemical shifts are sensitive indicators of protein structure and electrostatic perturbations due to the polarizability of the NH bond. $^1H,^{15}N$ HSQC spectra of Sac7d were collected as a function of pH with and without 0.3 M KCl (Fig. 4). In the absence of salt, significant unfolding was observed at pH 2 as indicated by collapse of the chemical shift dispersion in both the ^1H and ^{15}N dimensions. In the presence of salt, the majority of the ^1H and ^{15}N amide chemical shifts showed little change from pH 0 to 7.2 indicating no significant difference in Sac7d structure. Indeed, the HSQC spectra in the presence of 0.3 M KCl at pH 2 and 0 are identical, except for the loss of a few peaks due to more rapid chemical exchange at the lower pH. The NMR linewidths are consistent with monomeric native, acid-, and salt-induced folded forms. This is further supported by monomeric two-state unfolding for all three species (McCrary et al., 1996). We conclude that the structures of the acid-induced folded state at pH 0 and the salt-induced form at pH 2 are identical.

We focus here on pH-dependent ^1H chemical shift changes greater than 0.1 ppm and ^{15}N shifts greater than 1 ppm in the presence of salt with the intent of comparing the acid- and salt-induced folded states to the native state. Briefly, the largest change in the amide ^1H chemical shifts induced by decreasing pH in the presence of salt occurred at the C-terminal Lys66, which shifted downfield ($\Delta\delta_{NH} = +0.43$ ppm) due to an "intrinsic titration shift" (Bundi & Wüthrich, 1979) reflecting through-bond inductive effects due to the titration of the C-terminal carbonyl with an apparent pK of 3.2. The next most significant changes occurred in the connecting 3_{10} helix between the β-ribbon and the following three-stranded sheet (Ser18, $\Delta\delta_{NH} = -0.92$ ppm), in the loop between strands 2 and 3 of the sheet (Asn37, $+0.54$ ppm; Gly38, -0.70 ppm), and also in the N-terminal NH of the α-helix (Glu53, -0.79 ppm). The largest changes in ^{15}N chemical shift occurred in the same locations, i.e., the amide nitrogen of the C-terminal Lys66, which shifted upfield ($\Delta\delta_N = -5.4$ ppm), in the connecting 3_{10} helix (Ser18, -2.6 ppm), and then in the open loop (Asp36, -3.77 ppm; and Asn37, $+3.1$ ppm).

A closer look at the changes in the chemical shifts as a function of pH provides some insight into the effect of pH (Fig. 5; Table 1).
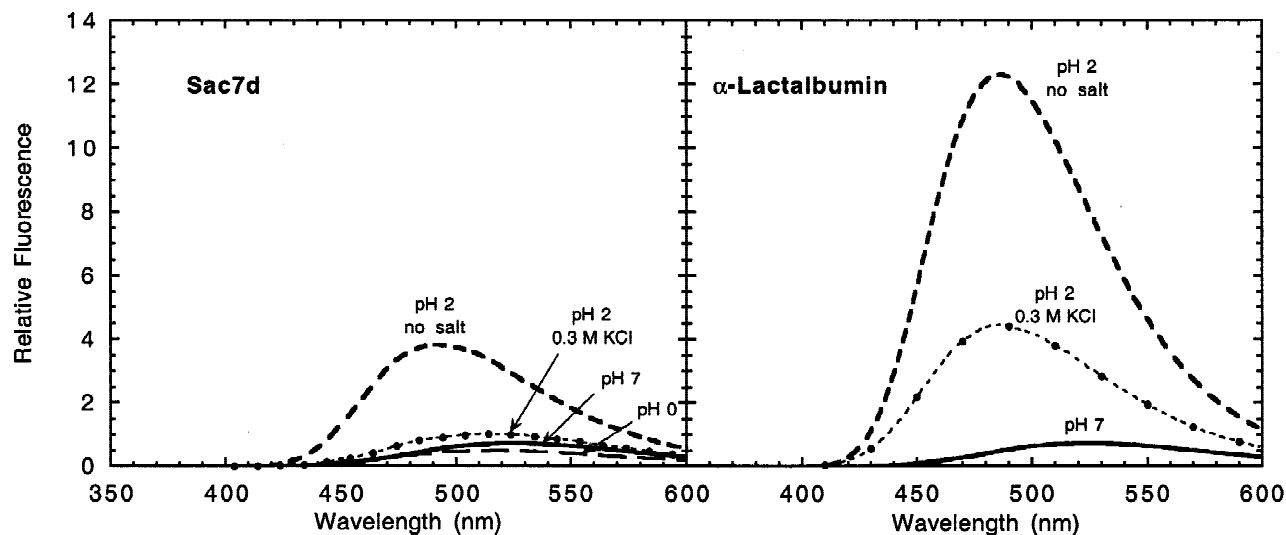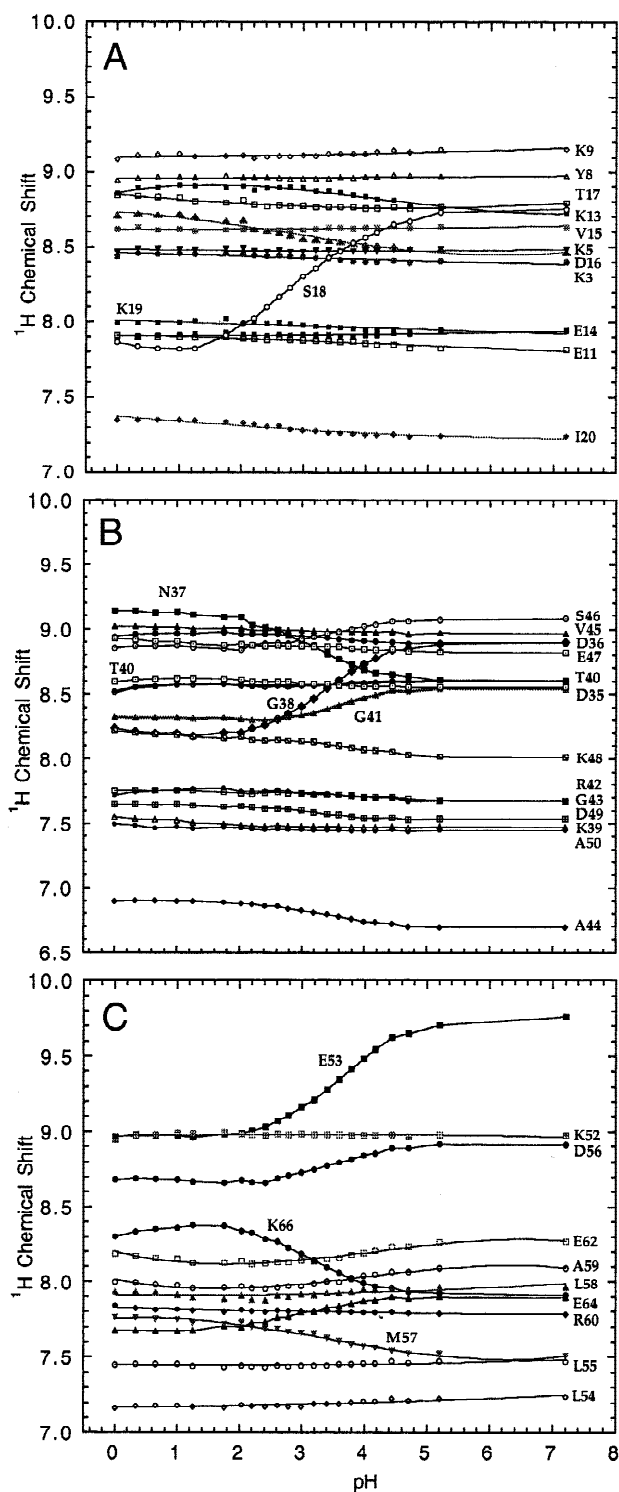

Fig. 3. Fluorescence emission spectra of ANS in the presence of Sac7d and α-lactalbumin at pH 7, 2, and also at pH 0 for Sac7d. All spectra were collected with 1 μM protein and 250 μM ANS at 25 °C. The emission spectrum of ANS in the absence of protein was insensitive to pH and salt and was similar to that observed at pH 7 in the presence of Sac7d or α-lactalbumin.
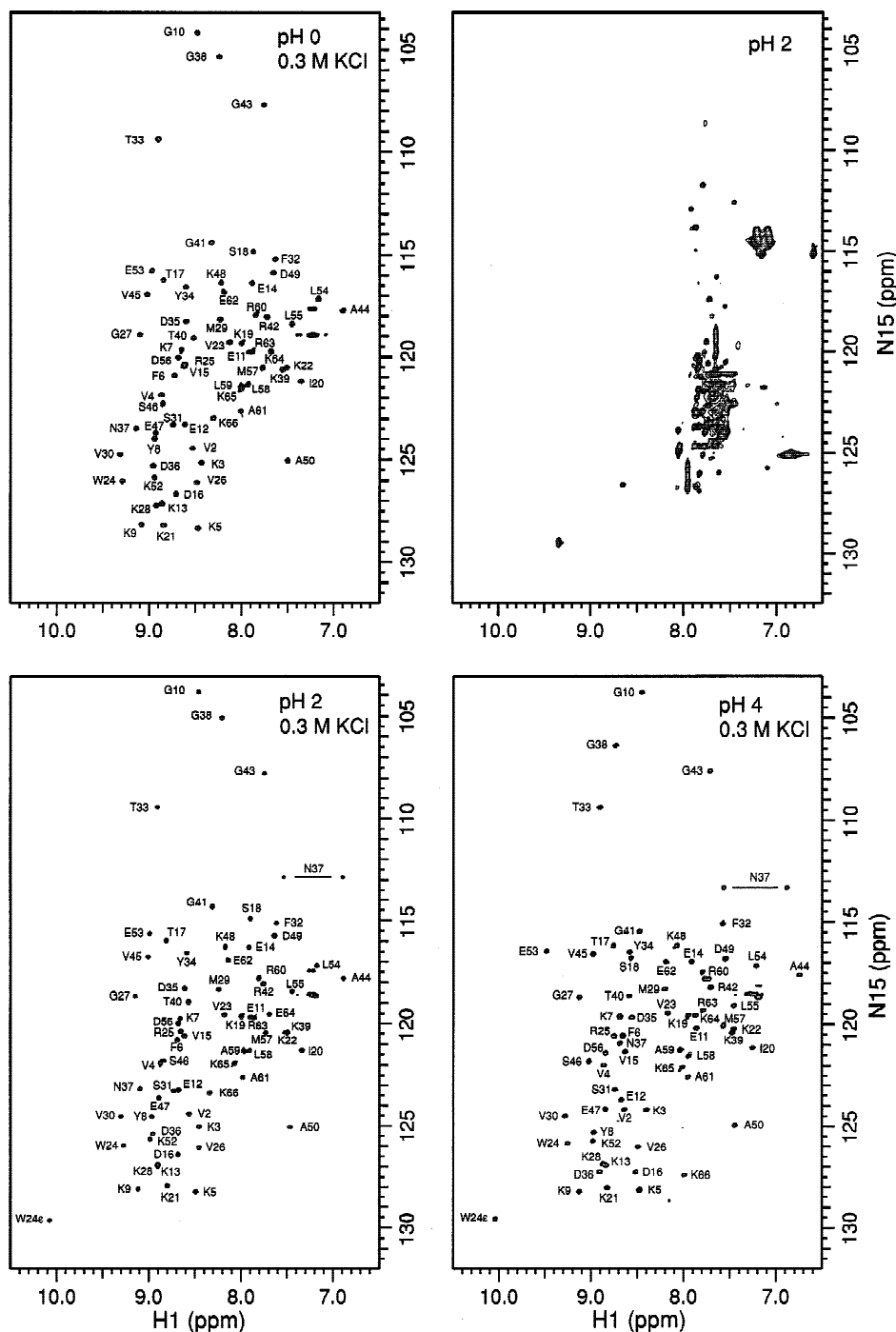
Fig. 4. ^{1}H,^{15}N HSQC spectra of Sac7d at pH 0 with 0.3 M KCl, pH 2 with no added salt, pH 2 with 0.3 M KCl, and pH 4.0 with 0.3 M KCl. All spectra were collected at 30 °C. Assignments are indicated by residue type and number. The side-chain NH$_2$ protons of the single asparagine (N37) are connected by a horizontal line. The NH$^{\epsilon 1}$ proton of the single tryptophan (W24) appears in the lower left corner of the spectra at pH 2 and 4. Neither the asparagine NH$_2$ or the W24 NH$^{\epsilon 1}$ protons could be observed at pH 0 due to fast exchange with solvent.

In the amino terminal β-ribbon, a very small effect of pH on the NH and N chemical shifts of Glu11, Glu12, and Glu14, was observed, with the magnitude and direction of the pH induced shift consistent with through-bond inductive effects (Bundi & Wüthrich, 1979). These data indicate that the effect of titration of these acidic residues has little effect on the structure of the protein in this region and the apparent pKs are approximately 3.7 to 4.1. As indicated above, the first residue in the sequence with a significant perturbation was at Ser18 with a large upfield shift (-0.92 ppm) of the NH with decreasing pH (Fig. 5A). The apparent pK indi-

Fig. 5. Representative effects of pH on the amide ^{1}H chemical shifts of residues in **(A)** the amino terminal β-ribbon and following 3_{10} helix, **(B)** the central β-sheet (D35-A50), and **(C)** the C-terminal α-helix.

Table 1. *Amide ^{1}H and ^{15}N chemical shift changes with apparent pKs observed for all acidic and other significantly affected residues*

Residue	H		N	
	$\Delta\delta_{NH}$[a]	pK_{app}[b]	$\Delta\delta_N$	pK_{app}
β-Turn				
Glu11	+0.089	3.97 (0.58)	−1.14	4.10 (0.91)
β-Ribbon strand 2				
Glu12	(<0.02)	—	−0.73	3.70 (0.98)
Lys13	+0.17	4.35 (0.86)	+1.21	4.82 (1.4)
Glu14	(<0.05)	—	−1.43	4.10 (0.66)
Connecting 3_{10} helix				
Asp16	+0.25	2.54 (0.59)	−1.1	2.81 (0.94)
Ser18	−0.92	2.96 (0.7)	−2.60	2.93 (0.68)
Loop between β-sheet strands 2 and 3				
Asp35	+0.061	2.97 (0.94)	−1.85	3.4 (0.86)
Asp36	+0.074	3.50 (1.18)	−3.77	3.11 (0.72)
Asn37	+0.54	3.15 (0.77)	+3.10	3.21 (0.78)
Gly38	−0.70	3.41 (0.93)	−1.63	3.46 (0.99)
β-Sheet strand 3				
Gly41	−0.22	3.66 (1.4)	−1.60	3.58 (1.15)
Ala44	+0.21	3.34 (0.71)	+0.37	3.72 (0.85)
Ser46	−0.22	3.46 (0.93)	(<0.5)	—
Connecting 3_{10} helix				
Glu47	(<0.10)	—	−1.33	4.13 (0.90)
Asp49	+0.11	3.07 (0.82)	−1.48	3.52 (0.90)
α-Helix				
Glu53	−0.79	3.62 (0.80)	−1.23	3.67 (0.89)
Leu55	(<0.04)	—	−0.94	3.41 (0.84)
Asp56	−0.24	3.56 (1.06)	−1.82	3.44 (1.11)
Met57	+0.26	3.30 (0.57)	+0.53	2.50 (0.58)
Glu62	−0.12	4.10 (1.47)	(<0.3)	—
Glu64	−0.23	2.94 (0.76)	(<0.1)	—
Lys66	+0.43	3.22 (0.99)	−5.40	3.15 (0.79)

[a] Differences are the maximal change in chemical shift observed as a function of pH in 0.3 M KCl, expressed as $\delta_{AH} - \delta_A$, with a positive value indicating an downfield shift upon protonation.

[b] Apparent pKs are phenomenological parameters characterizing the pH dependence of the NH and ^{15}N chemical shifts. They represent titration of neighboring acidic groups, and not the amide proton. Numbers in parentheses are the apparent Hill coefficients, with a value of one expected for a single titrating group.

of a carboxyl group hydrogen bonded to the NH (Bundi & Wüthrich, 1979). The NH of Ser18 is solvent exposed and is probably hydrogen bonded to the carboxyl of Asp16, and thus its chemical shift most likely reflects the titration of Asp16. The reduced apparent pK indicated by the NH of Asp16 (i.e., 2.54–2.81) supports this interpretation.

None of the amide chemical shifts in the first and second strands of the β-sheet (Lys21 through Tyr34) were affected significantly by pH. This is a basic region of the sequence (3 lysines, 1 arginine) and contains no acidic residues. The next most affected resonances are solvent exposed and are located in the loop between the second and third strands of the three-stranded sheet composed of residues

cates a titrating group with a pK of about 2.8. Residues 16 through 19 are involved in a single turn of 3_{10} helix connecting the β-ribbon with the following three-stranded sheet. The size and direction of the pH-induced shift of Ser18 NH are consistent with the titration

36–40 (Fig. 5B). The carboxyl side chain of Asp35 is in close proximity to the NH of Asp36 as well as that of Gly38, and the carboxyl of Asp36 is hydrogen bonded to the NH of Asn37. The pKs of both aspartates appear to be around 3.2 to 3.4. In the third strand of the β-sheet that follows, some small but clear effects were seen for the NH protons of Gly41, Ala44, and Ser46, with the amide nitrogen shift of Gly41 showing a significant variation with pH. These effects are relatively small and do not appear to be derived from structural perturbations since the large ring current shifts observed for the $C_\alpha H$ of Gly41 and Gly43 are largely unaffected by pH (see below). In the succeeding 3_{10} helix, perturbations were observed for the nitrogen chemical shift of the amide nitrogen of Glu47 and Asp49 due to titration of the carboxyl side chains of these groups with magnitudes comparable to that seen for Glu11, Glu12, and Glu14 in the β-ribbon. Finally, the effect of decreasing pH on the amide chemical shifts of the α-helix were small except for the NH of Glu53 at the N-terminal of the helix and the C-terminal Lys66 (Fig. 5C). The size and direction of the pH-induced shift of Glu53 NH is that expected for an intraresidue hydrogen bond between a Glu NH and its own carboxyl side chain (Bundi & Wüthrich, 1979; Mayer et al., 1979). As noted above, the magnitude and direction of the pH-induced shift for the NH of Lys66 is that expected for through-bond induced effects from the terminal carboxyl.

Thus, the most significant differences between the native, acid-, and salt-induced folded state amide ^1H and ^{15}N chemical shifts were observed primarily at exposed amides and are attributed to titration of carboxyl groups hydrogen bonded to the affected amide protons. The terminal Lys NH is the primary exception and this can be explained by inductive effects. There is no evidence in the HSQC spectra for significant differences between the native structure and those of the acid- and salt-induced states.

Ring current shifts

Ring current effects are exquisitely sensitive to the structure and packing of aromatic side chains in proteins due to a strong dependence on both distance and orientation relative to the plane of the aromatic ring (Dwek, 1973; Williamson et al., 1992; Case & Wright, 1993). The side chains of two tyrosines and two phenylalanines are packed within the hydrophobic core of Sac7d (Fig. 1) and lead to significant ring current-induced shifts in adjacent residues (Edmondson et al., 1995). The chemical shifts of affected backbone and side-chain protons in Lys9, Lys13, Ile20, Ser31, Gly41, and Gly43 were monitored by two-dimensional (2D) DQF-COSY as a function of pH (Table 2); and the magnitude of the ring current shifts showed little change from pH 4.5 to 0 in 0.3 M KCl. The small changes indicate that the tertiary structure and core packing of the native, acid-, and salt-induced folded states of Sac7d are essentially identical.

Small angle X-ray scattering

Small angle X-ray scattering was used to measure the radius of gyration (R_g) of Sac7d as a function of pH in the absence of salt. The X-ray scattering profile of Sac7d in 0.01 M KH_2PO_4 (pH 7.0) was found to be typical of globular proteins with little dependence on protein concentration. Guinier plots (i.e., $\ln[(I(Q)]$ vs. Q^2) were linear at small Q (Fig. 6), and extrapolation to zero Q gave a molecular weight of 7,500, consistent with the protein being

Table 2. *pH Dependence of chemical shifts of Sac7d protons most affected by ring current interactions* [a]

Residue	Proton	Random coil[b]	^1H chemical shifts		
			pH 0	pH 2	pH 4
Lys9	α	4.36	3.68	3.67	3.63
	$\beta1$	1.76	1.52	1.52	1.51
	$\beta2$	1.85	1.76	1.78	1.80
	γ	1.45	0.47	0.49	0.55
	δ	1.70	0.78	0.80	0.82
Lys13	$\beta1$	1.76	0.35	0.35	0.36
	γ	1.45	1.02	1.05	1.03
Ile20	δ	0.89	0.044	0.062	0.043
Ser31	$\beta1$	3.88	—	2.00	2.09
	$\beta2$	3.88	—	2.45	2.42
Gly41	$\alpha1$	3.97	2.64	2.64	2.43
	$\alpha2$	3.97	4.28	4.26	4.22
Gly43	$\alpha1$	3.97	2.45	2.44	2.35
	$\alpha2$	3.97	3.97	3.96	3.84

[a] Chemical shifts are measured relative to internal DSS in 0.3 M KCl.
[b] Random coil values are taken from Wüthrich (1986).

monomeric. The slope of the Guinier plot indicates an R_g for Sac7d of 12.8 ± 0.3 Å at pH 7.

The distance pair-distribution function $P(r)$ calculated from the scattering curve of Sac7d (Fig. 7) is another indication of the shape and size of the scattering particle. The $P(r)$ function of Sac7d at pH 7 shows an approximately symmetrical peak characteristic of globular proteins with a maximum dimension d_{max} of about 35 Å. The second moment of $P(r)$ is a more reliable method of determining R_g than the Guinier approximation and gave an R_g of 12.4 ± 0.1 Å for Sac7d at pH 7.
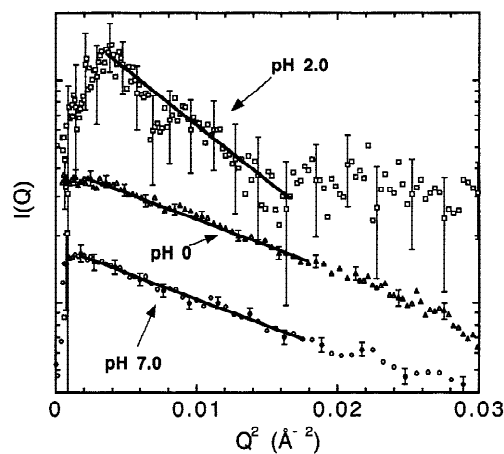
Fig. 6. Guinier plots of scattering data for Sac7d in 0.01 M KH_2PO_4 at pH 7.0 (bottom curve), at pH 0 (middle curve), and at pH 2.0 (top curve). The data were extrapolated to zero protein concentration. The curves are displaced for clarity. Error bars represent ± 1 S.D. The solid lines represent the fits to the Guinier approximation.

Fig. 7. $P(r)$ distribution functions of Sac7d protein at pH 7 (——), pH 2 (– – –), and pH 0.0 (– – – – –).

Discussion

Spectroscopic and scattering data demonstrate that the acid- and salt-induced folded states of Sac7d have a size and fold essentially identical to that of the native state. The methods utilized here are those commonly used to demonstrate the existence of a molten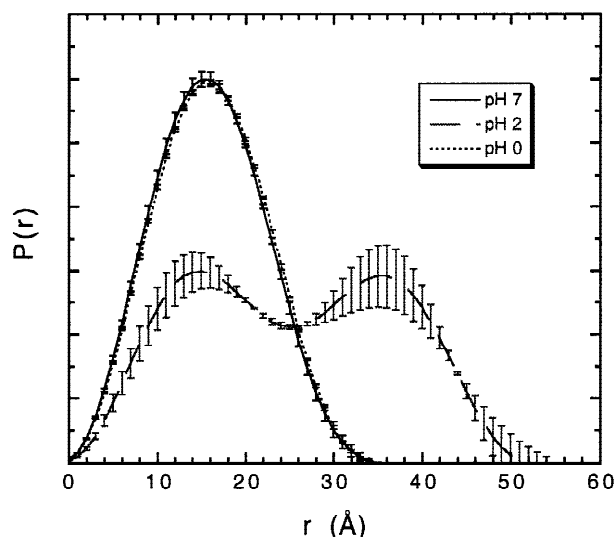 globule, which is typically indicated by a loss of the near-UV CD spectrum and reduced NMR chemical shift dispersion due to loss of tertiary interactions, enhanced ANS fluorescence enhancement due to the presence of hydrophobic surface area, and an expanded structure indicated by an increased radius of gyration (Kuwajima, 1989). Surprisingly, all of the data presented here indicates a native state under the conditions that are expected to create a molten globule in a protein that undergoes acid- and salt-induced folding.

The increased size of the molten globule relative to the native state is one of its most interesting and defining characteristics (Goto & Fink, 1989; Damaschun et al., 1991; Fink et al., 1993; Kataoka et al., 1993, 1995, 1997; Gast et al., 1994; Doniach et al., 1995; Eliezer et al., 1995; Semisotnov et al., 1996; Chen et al., 1996; Ikeguchi et al., 1997). For example, the acid molten globule of α-lactalbumin shows a 9% increase in R_g (from 15.7 to 17.2 Å) (Kataoka et al., 1997), apomyoglobin shows a 13% increase (17.5 to 19.7 Å) (Kataoka et al., 1995), and cytochrome c a 29% increase (13.5 to 17.4 Å) (Kataoka et al., 1993). The lack of expansion of the Sac7d acid-folded state relative to the N state (12.4 ± 0.1 Å for the native from the second moment of the $P(r)$ function, and 12.5 ± 0.1 Å for the acid folded state) is therefore taken as strong evidence against the acid-folded state being a molten globule.

The fluorescence enhancement of the dye ANS is also typically used as an indicator of a molten globule state (Mulqeen & Kronman, 1982; Goto & Fink, 1989; Semisotnov et al., 1991; Fink et al., 1994), presumably due to interactions with hydrophobic patches (Stryer, 1965). Typically, the fluorescence is unchanged in the presence of the native state, while the unfolded state leads to some enhancement, e.g., sixfold in parvalbumin (Fink et al., 1994) and twofold in β-lactamase (Goto & Fink, 1989). The sixfold enhancement observed here for acid unfolded Sac7d is consistent with these observations. The small enhancement observed for unfolded protein is sometimes given as an indication of partial structure in a thermally unfolded protein, since enhancement presumably results not only from the presence of hydrophobic groups, but also from hydrophobic patches. For this reason, a greater enhancement has been observed for the molten globule, e.g., about 14-fold in parvalbumin (Fink et al., 1994), 15-fold in β-lactamase (Goto & Fink, 1989), and an 18-fold enhancement observed here for α-lactalbumin. The negligible changes in ANS fluorescence observed for the acid- and salt-induced folded forms of Sac7d (1.5-fold enhancement for the salt-induced and 0.7 for the acid-induced form) therefore indicate that the acid- and salt-induced states are native like and not molten globular.

The remarkably large chemical shift dispersion observed here for amide ^{1}H and ^{15}N chemical shifts in the acid- and salt-induced folded state of Sac7d is similar to that seen for the native state and is in marked contrast to that seen for other protein A-states. For example, a significant loss in dispersion in ^{1}H chemical shifts upon formation of a molten globule, similar to that seen upon unfolding, has been observed for α-lactalbumin and ribonuclease H1 (Baum et al., 1989; Chamberlain & Marqusee, 1998), and pronounced collapse of the chemical shift dispersion of ^{1}H, ^{15}N HSQC spectra has been described upon molten globule formation for apomyo-

The R_g measured by X-ray scattering (12.4 Å) is in good agreement with that calculated from the NMR solution structure of Sac7d (entry 1sap in the Protein Data Bank) using the program HYDROPRO (de la Torre et al., 2000) with an atomic equivalent radius (AER) of 2.7 Å. The expected AER for proteins in vacuo is about 1.8 Å, and the difference (0.9 Å) is attributed to the hydration layer. The mean AER for proteins with molecular weights less than 100 kD is 2.6 ± 0.3 Å, and thus Sac7d does not appear to exhibit any unusual hydration effects.

The radius of gyration of Sac7d obtained from scattering data collected in low salt was found to be dependent on pH. At pH 2 in the absence of salt the R_g increased to 18.7 ± 1.0 Å as determined by the Guinier approximation, and 22.0 ± 0.2 Å as determined from the second moment of the $P(r)$. Further, the $P(r)$ distribution function indicated an expanded structure with a d_{max} of about 55 Å, consistent with a largely unfolded protein. The bilobal $P(r)$ is similar to that observed for a number of other unfolded proteins, and a Kratky plot, $I(Q) \times Q^2$ vs. Q (not shown), of the scattering data was consistent with an unfolded chain at pH 2 (Kataoka et al., 1997).

The scattering profile of Sac7d in 0.01 M KH_2PO_4 at pH 2 contained a large contribution from the interparticle structure factor, as indicated by a decrease in scattered intensity for low Q data (Fig. 6), and this effect could not be eliminated completely by extrapolating to zero protein concentration. At pH 2 repulsive forces between highly charged Sac7d proteins give rise to strong interparticle interference effects. Therefore, the R_g calculated for Sac7d at pH 2 may be underestimated, but this does not change the conclusion that the protein is mostly unfolded at pH 2 in the absence of salt.

At pH 0 the Guinier approximation indicates an R_g of 12.8 ± 0.2 Å, identical to that found for Sac7d at pH 7. Also, the $P(r)$ distribution function is identical within experimental error to that obtained at pH 7 with a d_{max} of 36 Å. The second moment of the $P(r)$ gives an R_g of 12.5 ± 0.1 Å for Sac7d at pH 0. These observations indicate that the acid-induced folded state has a R_g identical to the native state.

globin and α-lactalbumin (Eliezer et al., 1997, 1998; Kim & Baum, 1998).

We have previously demonstrated that the far-UV CD spectra of Sac7d indicate maintenance of the native secondary structure in the acid- and salt-induced folded states (McCrary et al., 1998). Titration of the protein from N to U and then to acid-folded state with decreasing pH in low salt leads to a well-defined isodichroic point in the far-UV CD, indicating only two states, N and U (i.e., the acid folded state is identical to N). Similarly, salt-induced folding at pH 2 also shows a single isodichroic point in the far-UV CD.

Molten globules typically show negligible thermal transitions upon unfolding by DSC (Yutani & Ogasahara, 1992; Griko et al., 1994; Griko & Remeta, 1999). The classic example is the total absence of an endotherm for α-lactalbumin at pH 2 where the acid molten globule is formed (Griko et al., 1994). In contrast, we have previously shown that thermal unfolding of both acid- and salt-induced folded Sac7d is a cooperative transition as indicated by a well-defined DSC endotherm (McCrary et al., 1996). The thermal unfolding of both the acid- and salt-induced folded states indicates that these unfold by a two-state transition as monomers. There is no evidence of aggregation of either species. In high salt (i.e., 0.3 M KCl) the T_m decreases with decreasing pH to reach a minimum of 58 °C ($\Delta H_{vh} = 41$ kcal/mol, $\Delta H_{cal} = 45$ kcal/mol) around pH 1.5. The T_m increases with a further decrease in pH to give a T_m of 63.3 °C at pH 0 ($\Delta H_{cal} = 44.4$, $\Delta H_{vh} = 44.7$ kcal/mol). The variation of T_m with pH has been shown to be consistent with the linkage of hydrogen ion and anion binding to a two-state N $\Leftrightarrow$ U unfolding reaction (McCrary et al., 1998).

As far as we are aware, Sac7d is the only protein described to date in which the acid unfolded chain is promoted into the native fold by either acid or salt. Fink et al. (1994) have proposed three classes of proteins in terms of their response to acid and salt. Type I refers to proteins (e.g., β-lactamase, apomyoglobin, cytochrome c) that unfold at low pH (e.g., pH 2) and then refold upon addition of salt to an A-state characterized by native-like secondary structure but little or no tertiary structure. Type II proteins (e.g., α-lactalbumin and carbonic anhydrase) directly form the A-state upon lowering pH without unfolding, and Type III proteins (including T4 lysozyme, chicken lysozyme, and ubiquitin) remain native-like and do not unfold or form an A-state down to pH <1. Type I proteins were further divided into three classes (A, B, and C) that differ in the extent of acid-induced unfolding and amount of structure in the A-state. In some respects, Sac7d resembles the type IC proteins (papain, parvalbumin, and ribonuclease A) that are partially unfolded with a decrease in pH; but acid or salt induce a molten globule in these proteins with little tertiary structure as indicated by loss of the near-UV CD spectrum. Ribonuclease A was an exception in this group and appears to behave more like Sac7d in that it regains most of its tertiary structure in the salt-induced folded state at pH 1.5. The results for Sac7d indicate that a fourth class, Type IV, is required in the Fink classification scheme in which the acid- and salt-induced folded states are identical to the native state. It remains to be seen if RNase A is also a member of this class.

The relative populations of the N, A, and U states for a protein that undergoes acid-induced folding have been summarized by a 2D phase diagram (Goto & Fink, 1990; Alonso & Dill, 1991) that describes the extent of folding as a function of pH and anion concentration. Goto and Fink (1990) proposed that the features of the phase diagram observed for apomyoglobin would be common

for all, or at least most, acid denatured proteins. The functional dependence of the extent of folding Sac7d on temperature, pH, and salt concentration has been previously obtained by fitting a wide array of CD and DSC data to a simple model that includes the linkage of two protonation and two anion binding reactions to protein folding (McCrary et al., 1998). We use this model here and the fitted parameters to construct a phase diagram for Sac7d by plotting the chloride concentration required to achieve 50% folding as a function of pH (Fig. 8). The phase diagram is similar to those observed experimentally and predicted for proteins forming acid unfolded states, except that the N-state region encompasses the expected A-state molten globular region.

It is not clear why Sac7d should demonstrate this unique ability to refold to the native state at low pH. As pointed out by Dill and Shortle (1991), understanding the forces responsible for formation of denatured and compact denatured states may be as difficult as determining those leading to the native state. It may be that the unique behavior of Sac7d is a result of it being highly basic. But a high pI seems an unlikely explanation since a basic protein would be even more positive at low pH and therefore less likely to fold properly. Cytochrome c is also very basic with a pI of 10.6, yet it is an "archetypal" Type IA protein in the Fink classification scheme.

Materials and methods

Sample preparation

Recombinant Sac7d was prepared as described previously (McAfee et al., 1995). Bovine α-lactalbumin (Sigma, St. Louis, Missouri) and ANS (Fluka, Buchs, Switzerland) were used without
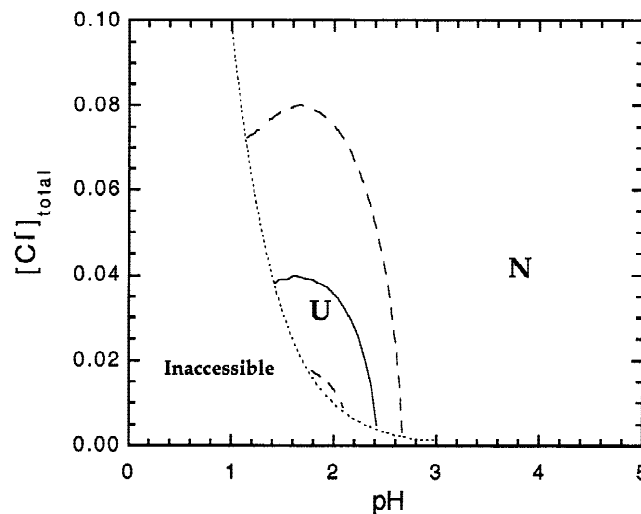
Fig. 8. Phase diagram for Sac7d as a function of pH and chloride ion concentration calculated from a linkage model containing two protonation sites and two anion binding sites linked to folding, with parameters obtained from fitting multidimensional (0–100 °C, pH 0–pH 8, 0–0.3 M KCl) DSC and folding progress surfaces followed by CD (McCrary et al., 1998). The pH is assumed to be adjusted with HCl. The solid line indicates the dependence of 50% unfolding on pH and chloride concentration, while the dashed lines indicate 25 and 75%. The dotted line indicates the upper limit of the region of the phase diagram inaccessible due to contribution of chloride by the acid.

further purification. Protein concentrations were determined spectrophotometrically using published extinction coefficients for Sac7d (McAfee et al., 1995) and α-lactalbumin (Kuwajima et al., 1985).

ANS fluorescence

Fluorescence spectra were collected with an SLM 8000C spectrofluorimeter with thermostated cell holders at 25 °C. The concentration of protein and ANS were 1 and 250 μM, respectively. Fluorescence emission spectra were obtained by excitation at 390 nm with a bandwidth of 1 nm for both excitation and emission. Sac7d and α-lactalbumin were dialyzed overnight against 1 mM glycine (pH 5.6) and diluted into the appropriate buffer for measurements at pH 2 and 7 (10 mM KH_2PO_4 at pH 7.0 or 1 mM glycine at pH 2.0). Concentrated HCl was used to adjust the pH to 0 using a glass pH electrode. Concentrated KCl (dissolved in the respective buffers) was used to adjust the salt concentration.

Small-angle X-ray scattering

Protein samples were concentrated with Centricon 3 (Amicon, Beverly, Massachusetts) concentrators to about 30 mg/mL and washed with 1 mM glycine buffer, pH 7.0 with repeated filling and centrifugation. Ailquots were dialyzed extensively against 0.01 M KH_2PO_4 adjusted with KOH or HCl to pH 7.0, 2.0, and 0.0 as measured with a pH glass electrode. The dialysate was used to dilute stock solutions of Sac7d to the appropriate concentration and to measure the scattering baseline.

Small angle X-ray scattering data were collected on beamline X12B at the National Synchrotron Light Source, Brookhaven National Laboratory using a MAR 300 image plate located 1.2 m from the quartz capillary tube sample holder. Scattering data were converted to $I(Q)$ vs. Q, where $I(Q)$ is the scattered X-ray intensity and Q is related to the scattering angle 2θ by $Q = 4\pi(\sin\theta)/\lambda$ where λ is the X-ray wavelength (1.5 Å). Scattering data were collected from $Q = 0.007$ to 0.35 Å^{-1}, and the net scattering was determined by subtraction of a normalized scattering profile of dialysate in the same sample cell. Scattering data were measured at 20 °C for protein samples ranging from 10 to 25 mg/mL, and scattering functions divided by concentration were linearly extrapolated to zero protein concentration (Pilz, 1982) using a least-squares singular value decomposition routine.

The vector length distribution functions $P(r)$ were calculated from the scattering data using an indirect Fourier transform as described elsewhere (Moore, 1980). The radius of gyration R_g was calculated from the second moment of $P(r)$ over the Q range of 0.04 to 0.26 for Sac7d at pH values of 7 and 0. The data for Sac7d at pH 2 exhibited interparticle interference effects that could not be corrected by extrapolating to zero protein concentration and was fit over the Q range of 0.06 to 0.28. R_g was also determined using the Guinier approximation to the low Q data ($Q < 0.13$).

The molecular mass of Sac7d was calculated from the small angle X-ray scattering data at zero scattering angle I_o and the relation

$$M_r = I_o \cdot M_s / I_{o,s}$$

where M_s and $I_{o,s}$ are the molecular weight and I_o values measured for a lysozyme standard.

NMR

Two-dimensional ^{1}H DQF-COSY NMR spectra were collected on a Varian VXR-S 500 MHz NMR spectrometer on 5 mM protein in 0.7 mL of 90% H_2O/10% D_2O at 30 °C. The pH was adjusted with concentrated HCl. Spectra were recorded in the phase-sensitive mode (Piatini et al., 1982; Rance et al., 1983) with the transmitter carrier frequency set on the water line (Zuiderweg et al., 1986), which was suppressed by presaturation with minimal power. Chemical shifts were referenced to DSS indirectly using the water chemical shift. ^{1}H, ^{15}N HSQC data were collected on 2.5 mM protein samples in 0.7 mL 90% H_2O/10% D_2O at 30 °C using a Varian INOVA 500 MHz NMR spectrometer with gradient selection of the ^{15}N magnetization and minimal perturbation of the water (Kay et al., 1992; Zhang et al., 1994). The salt concentration was adjusted with concentrated KCl, and the pH was adjusted with concentrated HCl. Typical data sets consisted of 512 t_1 increments with 1,024 complex data points in the t_2 dimension, with a ^{1}H spectral width of 6,000 Hz and an ^{15}N width of 1,700 Hz. Data were apodized with a shifted sine squared window function. ^{1}H chemical shifts were referenced to internal DSS, and the ^{15}N chemical shifts were calculated as described by Wishart et al. (1995). HSQC spectral assignments were obtained using a combination of 3D HSQC-NOESY and HSQC-TOCSY data (Zhang et al., 1994) and the previously obtained ^{1}H NMR assignments (Edmondson et al., 1995).

The pH dependence of the most affected resonances was quantified in terms of the size of the maximal change in chemical shift, an apparent pK, and a Hill coefficient by fitting the pH dependence of the observed chemical shift to the expression (Markley, 1975):

$$\delta_{obs} = = \delta_{A^-} \frac{1}{1 - 10^{n(\mathrm{pK}-\mathrm{pH})}} + \delta_{AH}\left(\frac{1}{1 - 10^{n(\mathrm{pK}-\mathrm{pH})}}\right)$$

where pK is that of the group (or groups) leading to the observed chemical shift perturbation, δ_{A^-} is the chemical shift of the high pH limit, δ_{AH} is the shift of the low pH limit, and n is the apparent Hill coefficient.

References

Alonso DOV, Dill K. 1991. Solvent denaturation and stabilization of globular proteins. *Biochemistry 30*:5974–5985.

Baldwin RL. 1991. Molten globules: Specific or nonspecific folding intermediates? *Chemtracts—Biochem Mol Biol 2*:379–389.

Baum J, Dobson CM, Evans PA, Hanley C. 1989. Characterization of a partly folded protein by NMR methods: Studies on the molten globule state of guinea pig α-lactalbumin. *Biochemistry 28*:7–13.

Brock T, Brock K, Belly R, Weiss R. 1972. *Sulfolobus*: A new genus of sulfur-oxidizing bacteria living at low pH and high temperature. *Arch Microbiol 84*:54–68.

Bundi A, Wüthrich K. 1979. Use of amide 1H-NMR titration shifts for studies of polypeptide conformation. *Biopolymers 18*:299–311.

Case DA, Wright PE. 1993. Determination of high-resolution NMR structures of proteins. In: Clore GM, Gronenborn AM, eds. *NMR of Proteins*. Boca Raton: CRC Press.

Chamberlain AK, Marqusee S. 1998. Molten globule unfolding monitored by hydrogen exchange in urea. *Biochemistry 17*:1736–1742.

Chen L, Hodgson KO, Doniach S. 1996. A lysozyme folding intermediate revealed by solution X-ray scattering. *J Mol Biol 261(5)*:658–671.

Damaschun G, Damaschun H, Gast K, Gernat C, Zirwer D. 1991. Acid dena-
tured apo-cytochrome c is a random coil: Evidence from small-angle X-ray
scattering and dynamic light scattering. *Biochim Biophys Acta 1078*:289–295.

de la Torre JG, Huertas ML, Carrasco B. 2000. Calculation of hydrodynamic
properties of globular proteins from their atomic-level structure. *Biophysi-
cal J 78*:719–730.

Dill KA, Shortle D. 1991. Denatured states of proteins. *Annu Rev Biochem
60*:795–825.

Doniach S, Bascle J, Garel T, Orland H. 1995. Partially folded states of proteins:
Characterization by X-ray scattering. *J Mol Biol 254(5)*:960–967.

Dwek RA. 1973. *Nuclear magnetic resonance (NMR) in Bbochemistry*. Oxford:
Clarendon Press.

Edmondson SP, Qiu L, Shriver JW. 1995. Solution structure of the DNA-binding
protein Sac7d from the hyperthermophile *Sulfolobus acidocaldarius*. *Bio-
chemistry 34*:13289–13304.

Eliezer D, Jennings PA, Dyson HJ, Wright PE. 1997. Populating the equilibrium
molten globule state of apomyoglobin under conditions suitable for struc-
tural characterization by NMR. *FEBS Lett 417*:92–96.

Eliezer D, Jennings PA, Wright PE, Doniach S, Hodgson KO, Tsuruta H. 1995.
The radius of gyration of an apomyoglobin folding intermediate. *Science
270(5235)*:487–488.

Eliezer D, Yao J, Dyson HJ, Wright PE. 1998. Structural and dynamic charac-
terization of partially folded states of apomyoglobin and implications for
protein folding. *Nat Struct Biol 5(2)*:148–155.

Fink AL. 1995. Compact intermediate states in protein folding. *Ann Rev Biophys
Biomol Struct 24*:495–522.

Fink A, Calciano L, Goto Y, Kurotsu T, Palleros D. 1994. Classification of acid
denaturation of proteins: Intermediates and unfolded states. *Biochemistry
33*:12504–12511.

Fink AL, Calciano LJ, Goto Y, Nishimura M, Swedberg SA. 1993. Character-
ization of the stable, acid-induced, molten globule-like state of staphylo-
coccal nuclease. *Protein Sci 2(7)*:1155–1160.

Finkelstein A, Shakhnovich E. 1989. Theory of cooperative transitions in pro-
tein molecules: II. Phase diagram for a protein molecule in solution. *Bio-
polymers 28*:1681–1694.

Freire E. 1995. Thermodynamics of partly folded intermediates in proteins.
Annu Rev Biophys Biomol Struct 24:141–165.

Garcia-Moreno EB. 1995. Probing structural and physical basis of protein en-
ergetics linked to protons and salt. *Methods Enzymol 259*:512–538.

Gast K, Damaschun H, Misselwitz R, Müller-Frome M, Zirwer D, Damaschun
G. 1994. Compactness of protein molten globules: Temperature-induced
structural changes of the apomyoglobin folding intermediate. *Eur Biophys J
23*:297–305.

Goto Y, Fink AL. 1989. Conformational states of β-lactamase: Molten globule
states at acidic and alkaline pH with high salt. *Biochemistry 28*:945–952.

Goto Y, Fink AL. 1990. Phase diagram for acidic conformational states of
apomyoglobin. *J Mol Biol 214*:803–805.

Goto Y, Nishikiori S. 1991. Role of electrostatic repulsion in the acidic molten
globule of cytochrome c. *J Mol Biol 222*:679–686.

Goto Y, Takahashi N, Fink A. 1990. Mechanism of acid-induced folding of
proteins. *Biochemistry 29*:3480–3488.

Griko Y, Freire E, Privalov PL. 1994. Energetics of the α-lactalbumin states: A
calorimetric and statistical thermodynamic study. *Biochemistry 33*:1889–1899.

Griko Y, Remeta D. 1999. Energetics of solvent and ligand-induced conforma-
tional changes in α-lactalbumin. *Protein Sci 8*:554–561.

Grote M, Dijk J, Reinhardt R. 1986. Ribosomal and DNA binding proteins of the
thermoacidophilic archaebacterium Sulfolobus acidocaldarius. *Biochim Bio-
phys Acta 873*:405–413.

Hagihara Y, Tan Y, Goto Y. 1994. Comparison of the conformational stability of
the molten globule and native states of horse cytochrome c. *J Mol Biol
237*:336–348.

Haynie D, Freire E. 1993. Structural energetics of the molten globule state.
Proteins 16:115–140.

Haynie DT, Freire E. 1994. Estimation of the folding/unfolding energetics of
marginally stable proteins using differential scanning calorimetry. *Anal Bio-
chem 216*:33–41.

Ikeguchi M, Kato S, Shimizu A, Sugai S. 1997. Molten globule state of equine
β-lactoglobulin. *Proteins 27(4)*:567–575.

Jennings PA, Wright PE. 1993. Formation of a molten globule intermediate
early in the kinetic folding pathway of apomyoglobin. *Science 262*:892–896.

Kataoka M, Hagihara Y, Mihara K, Goto Y. 1993. Molten globule of cytochrome-c
studied by small angle X-ray scattering. *J Mol Biol 229*:591–596.

Kataoka M, Kuwajima K, Tokunaga F, Goto Y. 1997. Structural characterization
of the molten globule of α-lactalbumin by solution X-ray scattering. *Protein
Sci 6*:422–430.

Kataoka M, Nishii I, Fujisawa T, Ueki T, Takunaga F, Goto Y. 1995. Structural
characterization of the molten globule and native states of apomyoglobin by
solution X-ray scattering. *J Mol Biol 249*:215–228.

Kay LE, Keifer P, Saarinen T. 1992. Pure absorption gradient enhanced hetero-
nuclear single quantum correlation spectroscopy with improved sensitivity.
J Am Chem Soc 114:10663–10665.

Kay MS, Baldwin RL. 1998. Alternative models for describing the acid unfold-
ing of the apomyoglobin folding intermediate. *Biochemistry 37*:7859–7868.

Kim S, Baum J. 1998. Electrostatic interactions in the acid denaturation of
α-lactalbumin determined by NMR. *Protein Sci 7*:1930–1938.

Kuwajima K. 1989. The molten globule state as a clue for understanding the
folding and cooperativity of globular-protein structure. *Proteins Struct Funct
Genet 6*:87–103.

Kuwajima K, Hiraoka Y, Ikeguchi M, Sugai S. 1985. Comparison of the tran-
sient folding intermediates in lysozyme and α-lactalbumin. *Biochemistry
24(4)*:874–881.

Kuwajima K, Nitta K, Yoneyama M, Sugai S. 1976. Three-state denaturation of
α-lactalbumin by guanidine hydrochloride. *J Mol Biol 106*:359–373.

Linderström-Lang K. 1924. The ionization of proteins. *Compt Rend Trav Lab
Carlsberg, Ser Chim 15*:29.

Markley J. 1975. Observation of histidine residues in proteins by means of
nuclear magnetic resonance spectroscopy. *Acc Chem Res 8*:70–80.

Matthew JB, Gurd FRN, Garcia-Moreno B, Flanagan MA, March KL, Shire
SJ. 1985. pH-Dependent processes in proteins. *CRC Crit Rev Biochem
18*:91–197.

Matulis D, Lovrien R. 1998. 1-Anilino-8-naphthalene sulfonate anion-protein
binding depends primarily on ion pair formation. *Biophysical J 74*:422–
429.

Mayer R, Lancelot G, Spach G. 1979. Side-chain-backbone hydrogen bonds in
peptides containing glutamic acid residues. *Biopolymers 18*:1293–1296.

McAfee J, Edmondson S, Datta P, Shriver J, Gupta R. 1995. Gene cloning,
sequencing, expression, and characterization of the Sac7 DNA-binding pro-
teins from the extremely thermophilic archaeon *Sulfolobus acidocaldarius*.
Biochemistry 34:10063–10077.

McCrary BS, Bedell J, Edmondson SP, Shriver JW. 1998. Linkage of proton-
ation and anion binding to the folding of Sac7d. *J Mol Biol 276*:203–224.

McCrary BS, Edmondson SP, Shriver JW. 1996. Hyperthermophile protein fold-
ing thermodynamics: Differential scanning calorimetry and chemical dena-
turation of Sac7d. *J Mol Biol 264*:784–805.

Moore PB. 1980. Small angle scattering: Information content and error analysis.
J Appl Crystallogr 13:168–175.

Mulqeen PM, Kronman MJ. 1982. Binding of naphthalene dyes to the N and A
conformers of bovine α-lactalbumin. *Arch Biochem Biophys 215*:28–39.

Ohgushi M, Wada A. 1983. "Molten-globule state": A compact form of globular
proteins with mobile side chains. *FEBS Lett 164*:21–24.

Oliveberg M, Vuilleumier S, Fersht A. 1994. Thermodynamic study of the acid
denaturation of barnase and its dependence on ionic strength: Evidence for
residual electrostatic interactions in the acid/thermally denatured state. *Bio-
chemistry 33*:8826–8832.

Piatini U, Sorensen O, Ernst R. 1982. Multiple quantum filters for elucidating
NMR coupling networks. *J Am Chem Soc 104*:6800–6801.

Pilz I. 1982. *Small-angle X-ray scattering*. New York: Academic Press.

Ptitsyn OB. 1987. Protein folding: Hypotheses and experiments. *J Prot Chem
6*:272–293.

Ptitsyn OB. 1995. Molten globule and protein folding. *Adv Prot Chem 47*:83–229.

Ptitsyn OB, Pain RH, Semisotnov GV, Zerovnik E, Razgulyaev OI. 1990. Ev-
idence for a molten globule state as a general intermediate in protein fold-
ing. *FEBS Lett 262*:20–24.

Rance M, Bodenhausen G, Wagner G, Ernst R, Wüthrich K. 1983. Improved
spectral resolution in COSY 1H NMR spectra of proteins via double quan-
tum filtering. *Biochem Biophys Res Comm 117*:479–485.

Sanz JM, Johnson CM, Fersht AR. 1994. The A-state of barnase. *Biochemistry
33*:11189–11199.

Semisotnov GV, Kihara H, Kotova NV, Kimura K, Amemiya Y, Wakabayashi K,
Serdyuk IN, Timchenko AA, Chiba K, Nikaido K, et al. 1996. Protein
globularization during folding. A study by synchrotron small-angle X-ray
scattering. *J Mol Biol 262(4)*:559–74.

Semisotnov GV, Rodionova NA, Razgulyaiv OI, Uversky VN, Gripas AF, Gil-
manshin RI. 1991. Study of the molten globule intermediate state in protein
folding by hydrophobic fluorescent probe. *Biopolymers 31*:119–128.

Stetter KO, Fiala G, Huber G, Huber R, Segerer A. 1990. Hyperthermophilic
microorganisms. *FEMS Microbiol Rev 75*:117–124.

Stigter D, Alonso DOV, Dill KA. 1991. Protein stability: Electrostatics and
compact denatured states. *Proc Natl Acad Sci USA 88*:4176–4180.

Stryer L. 1965. The interaction of a naphthalene dye with apomyoglobin and
apohemoglobin. A fluorescent probe for nonpolar sites. *J Mol Biol 13*:482–
495.

Tanford C. 1970. Protein denaturation. Part C: Theoretical models for the mech-
anism of denaturation. *Adv Prot Chem 24*:1–95.

Williamson MP, Asakura T, Nakamura E, Demura M. 1992. A method for the
calculation of protein alpha-CH chemical shifts. *J Biomol NMR 2(1)*:83–98.

Wishart DS, Bigam CG, Yao J, Abildgaard F, Dyson HJ, Oldfield E, Markley JL, Sykes BD. 1995. 1H, 13C, and 15N chemical shift referencing in biomolecular NMR. *J Biomol NMR 6*:135–140.

Wüthrich K. 1986. *NMR of proteins and nucleic acids*. New York: John Wiley.

Yang A-S, Honig B. 1993. On the pH dependence of protein stability. *J Mol Biol 231*:459–474.

Yang A-S, Honig B. 1994. Structural origins of pH and ionic strength effects on protein stability: Acid denaturation of sperm whale apomyoglobin. *J Mol Biol 237*:602–614.

Yutani K, Ogasahara K. 1992. Absence of the thermal transition in apo-α-lactalbumin in the molten globule state: A study by differential scanning calorimetry. *J Mol Biol 228*:347–350.

Zhang O, Kay LE, Olivier JP, Forman-Kay JD. 1994. Backbone 1H and 15N resonance assignments of the N-terminal SH3 domain of drk in folded and unfolded states using enhanced-sensitivity pulsed field gradient NMR techniques. *J Biomol NMR 4(6)*:845–858.

Zuiderweg E, Hallenga K, Olejniczak E. 1986. Improvement of 2D NOE spectra of biomacromolecules in H_2O solution by coherent suppression of the solvent resonance. *J Magn Res 70*:336–343.